Energy-Efficient for UAV-Assisted Vehicular Networks Under the Two-ways Street: Joint UAV Trajectory Optimization and Robust Power Control Approach

Zhixin Liu, Jianshuai Wei, Jiawei Su, Kit Yan Chan, Yazhou Yuan

***Abstract*—UAV-assisted Telematics mission offloading as an airborne base station is a promising solution, especially on two-way driving roads. This paper proposes a scheme to maximize energy efficiency in UAV-assisted Telematics and applies it to scenarios where both ground and Air Base Stations are present on two-way streets. However, the stability of the transmission for the offloading task can be seriously affected by the uncertain channel state. To model channel uncertainty, we employ a first-order Markov process and take into account the vehicle's mobility. Real-time optimization of UAV flight trajectory can improve the quality of service for auxiliary vehicle communication. Additionally, energy consumption is a crucial concern for UAVs in the system. The Dinkelbach method is used to solve non-convex fractional programming optimization problems while maximizing energy efficiency. A power control and UAV trajectory planning algorithm for maximizing energy efficiency is proposed to determine the optimal solution. Numerical simulations are performed to evaluate the algorithm's performance. The results demonstrate its effectiveness, particularly when compared to other UAV and one-way lane scenarios.**

***Index Terms*—Internet of Vehicle (IoV), Computation Offloading, Robust Power Control, Edge Computing, UAV Communication, Trajectory Optimisation**

I. Introduction

As the most promising solution for Intelligent Transportation Systems (ITS), the Internet of Vehicles (IoV) is expected to meet the rapidly growing demands of modern society, including those related to traffic efficiency, driving experience, and accident handling [1]. Unmanned aerial vehicle (UAV)-assisted vehicular networking can improve the energy efficiency of the system, and this paper proposes a scenario to maximize the energy efficiency of UAV-assisted vehicular network under Two-ways Street, however, the uncertain channel state can seriously affect the stability of data transmission, in order to consider the mobility of the vehicle and to simulate the uncertainty of the channel, In complex Two-ways Street scenarios, cooperation between the UAV and the ground base station can improve the utilization of system resources. A first-order Markov process can be used to plan the vehicles to select different time slots for communication with the receiver. To ensure high-quality communication, we implement probabilistic constraints on the signal link and use an integral transformation method to convert the original constraints into solvable ones. Additionally, we employ the Dinkelbach method to solve the non-convex robust optimization problem. To determine the optimal solution, we decompose the initial problem into three subproblems, which we solve through alternating iterations.

A scenario similar to the one in literature [2] for maximizing the energy efficiency of UAV-Assisted vehicular networks under Two-ways Street has been investigated [3], and in literature [4] the study The advantages of Two-ways Street communication are explored, vehicles vehicles traveling at high speed on a two-way highway [5], the ground base station is located on one side of the road, with the high speed of the vehicles traveling in the opposite direction [6], the vehicles traveling to the right will gradually move out of the current communication cell and cannot communicate with the ground base station, at this time, the UAV can be used as an airborne base station to receive the communication signal from the vehicles. The UAV flies parallel to the road at a fixed altitude without any obstacles, and our proposed algorithm can determine in real time how to select the communication object for the vehicle in the current time slot to maximize the energy efficiency of the system.

A. Related Works

Recently, air-ground integration has gained attention from industry and academia as a feasible solution to enhance wireless communication quality. UAVs are selected to assist the terrestrial network due to their flexible deployment, remote operation, and relay capability [7], [8], [9]. Some works have been devoted to an IoV edge computing network, consisting of a UAV-Assisted vehicular networks architectures, UAVs serve as edge computing servers, aerial base stations, or relays [10]. The authors in [11] took UAV transmitting its cached content files to vehicle users over UAV-to-Vehicle (U2V) links. In addition, the problem of UAV-assisted computation offloading is studied in [12], [13], where UAVs provide efficient computational services in vehicular computational offloading.

To enhance the flexibility of vehicle networks, UAVs can replace ground-based stations and provide aerial base station

Zhixin Liu, Jianshuai Wei, Jiawei Su and Yazhou Yuan are with the School of Electrical Engineering, Yanshan University, Qinhuangdao 066004, China. Emails: lzxauto@ysu.edu.cn, jswe@stumail.ysu.edu.cn, Sjw@stumail.ysu.edu.cn, yzyuan@ysu.edu.cn.

Kit Yan Chan is with the School of Electrical Engineering, Computing and Mathematical Sciences, Curtin University, Perth, Australia. Email: k-it.chan@curtin.edu.au.

This work is supported partly by National Natural Science Foundation of China under Grant 62273298, 62273295.

services to extend communication coverage to vehicles [14]. Meanwhile, optimizing the trajectory of the UAV can improve communication links between the unmanned aerial vehicle and other vehicles, particularly in environments where vehicles travel at high speeds in various directions. Yang et al. allocated resources and optimized the trajectory of the UAV in an energy-efficient UAV backscatter communication system in [15]. Optimizing the trajectory of the UAV can improve throughput, reduce energy consumption, and decrease latency [16].

The maximization of energy efficiency (EE) is a critical problem that requires a tradeoff between throughput and energy consumption to be solved. Some studies aim to decrease the energy consumption of UAVs through joint UAV trajectory design and resource allocation. Effective power control and altitude planning algorithms are required to maximize the energy efficiency of UAV-BS systems, and Aslani et al. reformulate the nonconvex problem into a convex problem using the Dinkelbach and alternating optimization methods in [17]. Wang et al. proposed an optimization problem to jointly determine subchannel allocation, optimize the UAV trajectory, and allocate power for each time slot to maximize system throughput [18]. Extensive attention and researches have been devoted to the area of air-ground integrated communications [7], [8]. The authors focus on the air-ground integrated network architecture design and resource management [7], [19]. In the heterogeneous cellular networks, the UAV is utilized to assist with emergency communications. A control framework that dynamically slices the spectrum resource for vehicular users is proposed in [8], where Lyapunov optimization theory is adopted. Nevertheless, despite the aforementioned works having sought to enhance the performance of AGHVNs, research into the integration of system robustness and resource allocation has not yet received sufficient attention. In [20], [21], the study investigated the advantages of bidirectional lane communication on highways where vehicles travel at high speeds and ground stations are located on one side of the road. As vehicles moving in the opposite direction travel at high speeds, vehicles moving to the right will gradually leave the current communication cell and will not be able to communicate with ground base stations. In such cases, UAVs can serve as aerial base stations to receive vehicle communication signals, it is evident from the preceding discussion that optimizing the trajectory of UAVs and controlling their power is essential for energy-efficient UAV-assisted vehicular networks.

Motivated by these points, we study the problem of system EE maximization in a UAV-assisted Vehicular communication network. The paper proposes a scheme to maximize energy efficiency in vehicular networking by using UAV assistance for task offloading.

B. Contributions

The scheme is designed for vehicles dynamically traveling on two-way streets. Unlike existing studies that consider fixed base stations in one-way lanes, this paper investigates a network system that places great emphasis on UAV trajectory optimization in cooperation with power control. The scheme ensures the quality of vehicular communication through outage probability constraints. To summarize, this paper's primary contributions can be outlined as follows:

- An optimal vehicular communication scheme is proposed by integrating UAV-assisted vehicular communication with task offloading. This scheme efficiently finds the vehicle-selected offloading base station in Two-ways Street through UAV trajectory optimization.
- The first-order markov process is used to handle the channel uncertainty caused by the high-speed movement of the vehicular network environment. Probabilistic constraints are employed to ensure vehicle QoS, and an integral transform approach is used to approximate non-convex probabilistic constraints in large-scale dynamic vehicular network environments.
- By optimizing the transmit power of the vehicle, the trajectory optimization of the UAV, and the allocation of time slots, and by proposing a scheme to transform the nonconvex problem using Dinkelbach's algorithm, the energy efficiency of the system is successfully maximized.

The rest of this paper is organized as follows: the model energy efficiency in vehicular networking by using UAV assistance for task offloading is presented in Section II. In Section III, the objective function and the non-convex constraints are formulated, and the problem solutions are proposed. In Section IV, the performance evaluations are presented. Finally, we conclusion the paper in Section V.

II. System model

The system model is shown in Fig. 1, we consider an integrated celestial and terrestrial network in which vehicles travel on a bidirectional highway and UAVs take off from the vicinity of the base station and cache the resources provided by the base station for download by the vehicles on the road, since it is a bidirectional lane, The base station is located at the origin of the coordinates at a height of h_0, and the D_R represents the radius length of the coverage of the roadside cell.To consider a more realistic road scenario, we model the vehicle motion as a constant velocity motion model [22]. We specify right as the positive direction and define the lane index $L = 1$ as the vehicle travelling to the right and $L = -1$ as the vehicle travelling to the left. Due to the fixed location of the base station, with the passage of time, there is inevitably a direction of the vehicle will be far away from the base station, which will inevitably affect its access to information from the base station. In order to decide whether the vehicle on the road needs to obtain information from the drone or the base station, we based on the channel state information predicted by the first-order Markov process from the vehicle to the base station and the channel state information obtained by the vehicle and the aerial base station drone line-of-sight link to the vehicle and the two data in the middle of the communication of the signal-to-noise ratio, respectively, the vehicle will select the party with the larger signal-to-noise ratio to request resources, $x_m[t] = 1$ for the vehicle to select the UAV for communication, and vice versa for the vehicle to select the base station for communication.

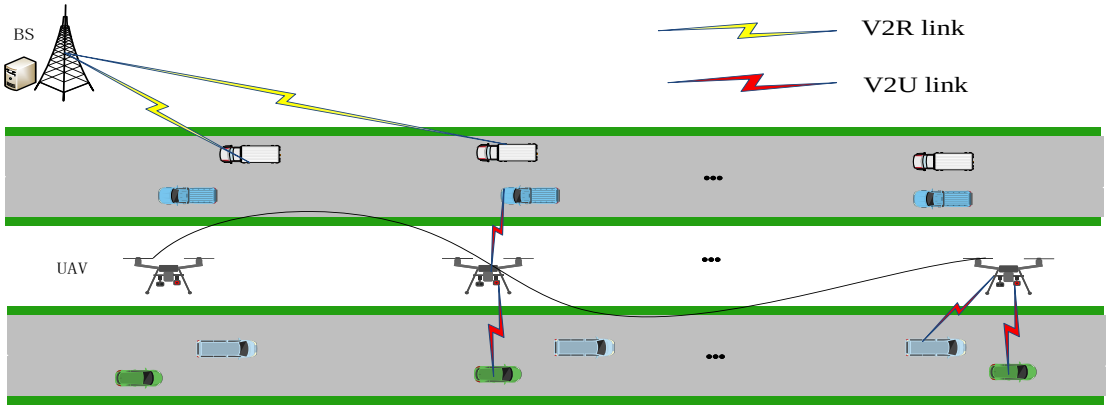

Fig. 1: UAV-Assisted Vehicular Networks model.

In the time slot t, the horizontal coordinates of the drone are $q_U[t] = \{\pi_u[t], \varpi_u[t]\}$. The UAV is flying unobstructed at a height of H from the road surface with a maximum speed of V_{max} and the initial horizontal position of the vehicle M is $q_m[0] = \{\pi_0, \varpi_0\}$. Assuming that the vehicle is travelling at speed ν_m in a uniform straight line, based on the previously defined lane index it can be derived that the vehicle M at the tth moment of the water The horizontal position changes to $\pi_m[t] = \pi_0 + l\nu_m t$, and the horizontal position of vehicle M is $q_m = \{\pi_m[n], \varpi_0\}$. Based on the position information we can get the distance information at the tth moment The distance between vehicle M and the roadside unit at t time slot is $d_{m,R}[t] = \|q_M[t] - q_R\| = \sqrt{\pi_m[t]^2 + {\varpi_0}^2 + H^2}$,The distance of vehicle M from the UAV at t time slot is $d_{m,U}[t] = \|q_M[t] - q_U[t]\| = \sqrt{(\pi_m[t] - \pi_u[t])^2 + (\varpi_m[t] - \varpi_u[t])^2 + H^2}$. Furthermore, some notations used in this paper are given in Table I.

TABLE I: Notations

$\Pr\{\cdot\}$	Probability function.
$\mathrm{q}[t]$	UAVs position at slot t.
$\mathbb{R}^k$	Set of k-dimensional real vectors.
$\mathbf{q}$	Index set of UAV trajectory $\mathbf{q}$=$[q_1, \cdots, q_i, \cdots, q_M]$.
$\mathbf{p}$	Index set of vehicle power $\mathbf{p}$=$[p_1, \cdots, p_i, \cdots, p_M]$.
$\mathcal{T}$	Index set of time slot $\mathcal{T}$=$\{1, 2, \cdots, T\}$.
$\mathcal{M}$	Index set of all active vehicles $\mathcal{M}$=$\{1, 2, \cdots, M\}$.
$\mathrm{E}\{\cdot\}$	Expected value of a random variable.

A. Channel and Energy Consumption Models of V2R Communication

Due to the fast movement of the vehicle, a first-order Markov process is constructed for the V2R communication between the vehicle and the roadside device, where the channel state information at the tth instant is predicted based on the state prediction at the previous instant. i.e.

$$h_m = \widetilde{h}_m^2 + \hat{h}_m^2, \tag{1}$$

here $\widetilde{h}_m$ is an observation and $\hat{h}_m$ is an exponential distribution obeying the parameter $a = \frac{1}{L_{i,j}^k{}^2(1-\zeta_{i,j}^k{}^2)}$ [23]. The signal-to-noise ratio (SNR) of the mth vehicle received by the ground base station at the tth time slot can be expressed as:

$$\gamma_{m,R}[t] = \frac{p_m[t] h_{m,R}[t]}{\sigma^2} \tag{2}$$

According to Shannon's capacity theorem, the transmission rate from the vehicle to the terrestrial base station can be expressed as follows:

$$R_{m,R}[t] = \log_2(1 + \gamma_{m,R}[t]). \tag{3}$$

The amount of data transmitted from the vehicle to the terrestrial base station can be expressed as,

$$L_{m,R} = B_0 \sum_{m=1}^{M} \sum_{t=1}^{T} x_m[t] R_{m,R}[t], \tag{4}$$

where B_0 denotes the bandwidth, $x_m[t] = 1$ indicates that the vehicle decides to transmit data to the terrestrial base station at this time, and $x_m[t] = 0$ conversely indicates that the vehicle decides to transmit data to the UAV base station at this time.

$$E_{m,R} = \sum_{m=1}^{M} \sum_{t=1}^{T} x_m[t] p_m[t] \tag{5}$$

B. Channel and Energy Consumption Models of V2U Communication

For the communication between the vehicle and the UAV without obstacle occlusion in the middle, which is a line-of-sight link, an airborne RF link model is constructed, and the channel gain from the m vehicle to the UAV at tth time slot is,

$$h_{m,U}[t] = \frac{\varsigma_0}{d_{m,U}[t]^2} \tag{6}$$

Here the symbol ς_0 represents the power gain per unit distance of one metre. With the aforementioned information in mind, the transmission rate from the unmanned aerial vehicle (UAV) to the vehicle can be calculated as:

$$R_{m,U}[t] = \log_2(1 + \gamma_{m,U}[t]), \tag{7}$$

$$\gamma_{m,U}[t] = \frac{p_m[t]\, h_{m,U}[t]}{\sigma^2}, \tag{8}$$

the SNR of the vehicle-to-UAV communication is denoted by the symbol. The amount of data transmitted by the vehicle to the UAV airborne base station can be expressed as,

$$L_{m,U} = B_0 \sum_{m=1}^{M} \sum_{t=1}^{T} x_m R_{m,U}[t], \tag{9}$$

where the bandwidth, denoted by B_0, is used to calculate the transmission energy consumption of a vehicle communicating with an airborne base station UAV.

$$E_{m,U} = \sum_{m=1}^{M} \sum_{t=1}^{T} y_m[t]\, p_m[t] \ . \tag{10}$$

Given the existence of a robust line-of-sight link between the UAV and the roadside unit, it is postulated that the data transmitted from the vehicle to the UAV can be efficiently transmitted to the ground base station and processed by the edge server attached to the roadside unit.

C. Vehicle Computing Task Offloading and Energy Model

The edge server connected to the roadside unit is capable of performing data computational processing on the received vehicle data. Consequently, the computational offloading process necessitates the utilisation of computational resources to execute the subtasks divided by the collaborative computational model. The computational task for the mth vehicle is denoted as A_m. At a specific time interval, when the task is split to the roadside unit, it is denoted as $A_{R,m} = z_m A_m$. The computation time can be expressed as:

$$t_m^{mec} = \frac{A_{R,m}}{f_R} \tag{11}$$

The time taken by the vehicle to complete the task upload and computation is the sum of the fixation time, which is the period of time required for the roadside unit to send data to the edge server, and the computation time. In order to ensure the smooth transmission of the task and its computation, the computation time should be less than the travelling time of the vehicle within the unit's coverage area.

The computational energy consumption of the edge server subsequent to the mth sub-task is as follows:

$$E_m^{mec} = \aleph A_{R,m} {f_R}^2 \tag{12}$$

where the effective switching capacitance of the CPU, denoted by the symbol $\aleph$, is greater than zero, this value depends on the specific chip architecture.

D. Problem Formulation

In this section, we formulate the energy efficiency maximisation problem for UAV-assisted two-way lane vehicles. Our objective is to maximise the total energy efficiency of the system by jointly optimising the transmit power of the vehicles on the two-way lanes as well as the trajectory of the UAV. First, we define the energy efficiency of this network communication system.

$$EE(\mathbf{P}, \mathbf{Q}, \mathbf{X}) = \frac{L_m(\mathbf{P}, \mathbf{Q}, \mathbf{X})}{E_m(\mathbf{P}, \mathbf{X})} \tag{13}$$

The total amount of data sent by the vehicle to the ground base station and the air base station is given by $L_m = L_{m,R} + L_{m,U}$. The energy consumption of the vehicle and the air base station of the ground base station, as well as the computational energy consumption of the edge server, is included in the term E_m. Given that energy consumption will occur during the flight of the unmanned aerial vehicle (UAV), it is important to consider this when evaluating the energy consumption of the vehicle in communication with the UAV. Additionally, the energy trade-off between the communication with the air base station and the ground base station should be taken into account. Consequently, the total power consumption of the system is expressed as $E_m = E_m^{mec} + (1-\theta)E_{m,R} + \theta E_{m,U}$, where $0 \le \theta \le 1$ represents the weighting coefficient of the energy cost of the vehicle when communicating with the UAV. When θ is larger, it signifies that greater consideration is given to the energy cost of the UAV. The system energy efficiency maximisation problem is formulated as follows:

$$\begin{aligned}
\mathbf{P}: \quad & \max_{\mathbf{P},\mathbf{Q},\mathbf{X}} EE(\mathbf{P}, \mathbf{Q}, \mathbf{X}) && (14)\\
\text{s.t.} \quad & \Pr\{x_m[t]\,\gamma_{m,R}[t] + y_m[t]\,\gamma_{m,U}[t] \ge \gamma_{th}\} \\
& \ge 1-\varepsilon_3, \forall m, t && (14\text{-}1)\\
& 0 \le p_m[t] \le p_{max}, \forall m && (14\text{-}2)\\
& x_m[t] + y_m[t] = 1, \forall m && (14\text{-}3)\\
& \frac{D_R}{\nu_m} \ge t_m^{mec} + t_{wired} && (14\text{-}4)\\
& q_U^{n+1} - q_U^n \ \le tV_{max}, \forall m && (14\text{-}5)
\end{aligned}$$

The (14-1) in the aforementioned equation represents the interruption probability constraint, which is designed to guarantee the quality of service by ensuring vehicle communication. The (14-2) represents the constraint on the maximum and minimum transmit power of the vehicle, The equation (14-3) demonstrates that the task of each vehicle at any given moment in time can only be offloaded to either the UAV or the terrestrial base station. The threshold of the signal-to-noise ratio, denoted by γ_{th}, is a fixed value, (14-4) represents the necessity to dispatch the vehicle before it leaves the roadside cell coverage area. Prior to the server completing the computation of completion data and the allocation of time slot resources, this constraint can be employed. The time point t_{wired} is defined as the time at which the roadside unit transmits data to the edge server for a fixed duration. The flight trajectory of the UAV is constrained by the inequality given in Equation 14-5, which states that the actual distance flown by the UAV per second must be less than or equal to the maximum flyable distance of the UAV.

III. Solving the EE Maximization Problem

In this section, the energy efficiency maximisation problem from the previous section is broken down into two subproblems to be solved. For the fractional programming which

is difficult to solve, it can be solved by using Dinkelbach's method to transform it into an easy-to-solve reduced-form programming. The vehicle's launch power should first be fixed, after which the UAV's flight trajectory can be solved. This process is then repeated for the UAV's flight trajectory, with the vehicle's launch power being fixed in each iteration. This alternating process of optimisation continues until the algorithm converges. It should be noted that question (14) in the previous section is a non-convex problem. In order to deal with this problem efficiently, we propose a joint power allocation and UAV trajectory planning scheme which decouples the problem (14) into three subproblems. [24].

A. Probabilistic Constrained Approximation and Optimal Power Control Problems

In the preceding section of the equation (14-1), it was demonstrated that the vehicle's power in the context of probabilistic constraints is challenging to resolve directly. In this instance, the integral transformation will be employed to transform the complex probability constraint problem into a simpler form.

Theorem 1. *For (14-1), the interruption probability constraints of vehicle users*

$$\Pr\left\{x_m\left[t\right]\gamma_{m,R}\left[t\right]+y_m\left[t\right]\gamma_{m,U}\left[t\right]\geq\gamma_{th}\right\}\geq 1-\varepsilon_3$$

Equivalent:

$$\begin{aligned} &p_m\left[t\right]x_m\left[t\right]\ln\left(1-a\varepsilon_3\right)+\left(\gamma_{th}-y_m\left[t\right]\gamma_{m,U}\right)\left[t\right]a\sigma^2 \\ &\qquad\leq ap_m\left[t\right]x_m\left[t\right]\hat{h}_m\left[t\right] \end{aligned} \tag{15}$$

Proof:

$$\frac{x_m\left[t\right]p_m\left[t\right]h_{m,R}\left[t\right]}{\sigma^2}\geq\gamma_{th}-y_m\left[t\right]\gamma_{m,U}\left[t\right] \tag{16}$$

$$\Leftrightarrow p_m\left[t\right]\widetilde{h}_m\left[t\right]\geq\frac{\left(\gamma_{th}-y_m\left[t\right]\gamma_{m,U}\left[t\right]\right)\sigma^2}{x_m\left[t\right]}-p_m\left[t\right]\hat{h}_m\left[t\right]$$

Therefore the vehicle user's interruption probability constraint makes a reformulation as follows:

$$Pr\left\{x_m\left[t\right]\gamma_{m,R}\left[t\right]+y_m\left[t\right]\gamma_{m,U}\left[t\right]\geq\gamma_{th}\right\}\geq 1-\varepsilon_3 \tag{17}$$

$$\Leftrightarrow\Pr\left\{\widetilde{h}_m\left[t\right]\geq\frac{\left(\gamma_{th}-y_m\left[t\right]\gamma_{m,U}\left[t\right]\right)\sigma^2}{p_m\left[t\right]x_m\left[t\right]}-\hat{h}_m\left[t\right]\right\}\geq 1-\varepsilon_3$$

Since the probability density function of the random variable $\widetilde{h}$ is $f_x=e^{-ax}$, it can be obtained by integral transformation:

$$\begin{aligned} &\int_0^{\frac{\left(\gamma_{th}-y_m\left[t\right]\gamma_{m,U}\right)\sigma^2}{p_m\left[t\right]x_m\left[t\right]}-\hat{h}_m\left[t\right]}e^{-ax}dx\leq\varepsilon_3 \\ &\Leftrightarrow p_m\left[t\right]x_m\left[t\right]\ln\left(1-a\varepsilon_3\right)+\left(\gamma_{th}-y_m\left[t\right]\gamma_{m,U}\left[t\right]\right)a\sigma^2 \\ &\quad\leq ap_m\left[t\right]x_m\left[t\right]\hat{h}_m\left[t\right] \end{aligned} \tag{18}$$

For ease of expression, we define $\gamma_{m,U}\left[t\right]=p_m\left[t\right]\eta_{m,U}\left[t\right]$the $\eta_{m,U}\left[t\right]=h_{m,U}\left[t\right]/\sigma^2$further $\kappa_m\left[t\right]=x_m\left[t\right]\ln\left(1-a\varepsilon_3\right)-y_m\left[t\right]\eta_{m,U}\left[t\right]a\sigma^2-ax_m\left[t\right]\hat{h}_m\left[t\right]$ Rewrite the equation (18) as.

$$p_m\left[t\right]\kappa_m\left[t\right]+a\sigma^2\gamma_{th}\leq 0 \tag{19}$$

The process of determining the vehicle's transmit power necessitates the execution of power rate allocation procedures in conjunction with UAV trajectory planning and a multitude of iterations. The subproblem pertaining to the vehicle launch power, $p_m\left[t\right]$, is elucidated as follows:

$$\max_{\mathbf{P}}=\frac{L_m\left(\mathbf{P}\right)}{E_m^{mec}+\left(1-\theta\right)E_{m,R}\left(\mathbf{P}\right)+\theta E_{m,U}\left(\mathbf{P}\right)} \tag{20}$$

$$\text{s.t. }(19),(14\text{-}2) \tag{20-1}$$

Notice that the problem (20) is a fractional planning problem. In order to transform it into a subtractive planning problem, it is proposed that it be solved using the Dinkelbach method.

$$\begin{aligned} F(\chi)=\max_{\mathbf{P}}&\sum_{t=1}^{T}\sum_{m=1}^{M}B_0x_m^{\{l\}}\left[t\right]\log_2\left(1+p_m\left[t\right]\eta_{m,R}^{\{l\}}\left[t\right]\right) \\ &-\chi\sum_{t=1}^{T}\sum_{m=1}^{M}\left(1-\theta\right)x_m^{\{l\}}\left[t\right]p_m\left[t\right]+\theta y_m^{\{l\}}\left[t\right]p_m\left[t\right] \\ &+\sum_{t=1}^{T}\sum_{m=1}^{M}B_0y_m^{\{l\}}\left[t\right]\log_2\left(1+p_m\left[t\right]\eta_{m,U}^{\{l\}}\left[t\right]\right) \end{aligned} \tag{21}$$

$$\text{s.t. }(19),(14\text{-}2) \tag{21-1}$$

$\eta_{m,R}^{\{l\}}\left[t\right]=h_{m,R}\left[t\right]/\sigma^2$ in the above equation. $\eta_{m,U}^{\{l\}}\left[t\right]=h_{m,U}\left[t\right]/\sigma^2$. Considered constant at every l iteration, for the convex problem (21). we can construct the Lagrangian function and apply the Lagrangian dyadic method to solve it:

$$\begin{aligned} &L\left(\mathbf{p},\lambda\right) \\ &=\sum_{t=1}^{T}\sum_{m=1}^{M}B_0x_m^{\{l\}}\left[t\right]\log_2\left(1+p_m\left[t\right]\eta_{m,R}^{\{l\}}\left[t\right]\right) \\ &+\sum_{t=1}^{T}\sum_{m=1}^{M}B_0y_m^{\{l\}}\left[t\right]\log_2\left(1+p_m\left[t\right]\eta_{m,U}^{\{l\}}\left[t\right]\right) \\ &-\chi\sum_{t=1}^{T}\sum_{m=1}^{M}\left(1-\theta\right)x_m^{\{l\}}\left[t\right]p_m\left[t\right]+\theta y_m^{\{l\}}\left[t\right]p_m\left[t\right] \\ &-\sum_{t=1}^{T}\sum_{m=1}^{M}\lambda_{m,t}\left(p_m\left[t\right]\kappa_m\left[t\right]+a\sigma^2\gamma_{th}\right) \end{aligned} \tag{22}$$

Where the Lagrange multiplier $\lambda_{m,t}\geq 0$, the Lagrange pairwise function of (22) is expressed as:

$$D(\lambda)=\max_{0\leq P_m[t]\leq P_{\max}}L\left(\mathbf{p_m},\lambda\right) \tag{23}$$

where the dyadic problem of (23) is:

$$\min_{\lambda_{m,t}\geq 0}D\left(\mathbf{p_m},\lambda\right) \tag{24}$$

The problem (24) is a convex problem and satisfies the Karush-Kuhn-Tucker (KKT) condition, which can be made to have a first-order derivative equal to zero in an analogous solution process using the KKT condition:

$$\begin{aligned} &\frac{B_0x_m^{\{l\}}[t]\eta_{m,R}^{\{l\}}[t]}{\ln 2\left(1+p_m[t]\eta_{m,R}^{\{l\}}[t]\right)}+\frac{B_0y_m^{\{l\}}[t]\eta_{m,U}^{\{l\}}[t]}{\ln 2\left(1+p_m[t]\eta_{m,U}^{\{l\}}[t]\right)}+\chi\left(\theta-x_m^{\{l\}}\left[t\right]\right) \\ &-\sum_{t=1}^{T}\lambda_{m,t}\left(-y_m[t]\eta_{m,U}[t]a\sigma^2+x_m[t]\hat{h}_m[t]-\frac{x_m[t]a\varepsilon_3}{1-a\varepsilon_3}\right)=0, \end{aligned} \tag{25}$$

From the above equation

$$p_m[t] = \frac{x_m^{\{l\}}[t]}{\eta_{m,R}^{\{l\}}[t]} + \frac{y_m^{\{l\}}[t]}{\eta_{m,U}^{\{l\}}[t]} - \frac{B_0}{\ln 2\lambda_{m,t}\left[y_m^{\{l\}}[t]\eta_{m,U}^{\{l\}}[t]a\sigma^2 + x_m^{\{l\}}\left(\hat{h}_m[t] - \frac{a\varepsilon_3}{1-a\varepsilon_3}\right)\right]} \tag{26}$$

For simplicity we make the $c_m[t] = y_m^{\{l\}}[t]\,\eta_{m,U}^{\{l\}}[t]\,a\sigma^2 + x_m^{\{l\}}\left(\hat{h}_m[t] - \frac{a\varepsilon_3}{1-a\varepsilon_3}\right)$ According to (25), the power allocation is iteratively updated by

$$p_m[t]^* = \left[\frac{x_m^{\{l\}}[t]}{\eta_{m,R}^{\{l\}}[t]} + \frac{y_m^{\{l\}}[t]}{\eta_{m,U}^{\{l\}}[t]} - \frac{B_0}{\ln 2\lambda_{m,t}c_m[t]}\right]_0^{p_{max}} \tag{27}$$

We can update the Lagrange multiplier λ_m using the subgradient method as follows:

$$\lambda_m^{(i+1)} = \left[\lambda_m^{(t)} + \Delta_m^{(t)} G_{\lambda_m}\right]^+ \tag{28}$$

where G_{λ_m} represents the step size of the Lagrange multiplier and $G_{\lambda_m} \geq 0$. The variable i is the iteration index and the positive part of the variable x is defined as $[x]^+ = \max[0, x]$. The Lagrange multipliers are updated by the subgradient method as follows:

$$G_{\lambda_m} = p_m[t]\,\kappa_m[t] + a\sigma^2\gamma_{th} \tag{29}$$

Algorithm 1 Power Allocation Algorithm

1: **Input:** Initialize variables $\mathbf{X}^{\{l\}}$, $\mathbf{Y}^{\{l\}}$and $\mathbf{Q}^{\{l+1\}}$, set $\chi(n) = 0$, $n = 1$ as iteration index and $\epsilon_1 > 0$ as accuracy threshold.
2: **repeat**
3: Obtain $p_n = p_m[t]^*$ by solving (27) with $\mathbf{X}^{\{l\}}$, $\mathbf{X}^{\{l\}}$, $\mathbf{Q}^{\{l+1\}}$ and ϵ_1.
4: Update $F(\chi(n)) = L_n\left(\mathbf{P}(\mathbf{n}), \mathbf{X}^{\{l\}}, \mathbf{Y}^{\{l\}}, \mathbf{Q}^{\{l+1\}}\right) - \chi(n)E_n\left(\mathbf{P}(\mathbf{n}), \mathbf{X}^{\{l\}}, \mathbf{Y}^{\{l\}}\right)$;
5: Update $F(\chi(n+1)) = \frac{L_n\left(\mathbf{P}(\mathbf{n}), \mathbf{X}^{\{l\}}, \mathbf{Y}^{\{l\}}, \mathbf{Q}^{\{l+1\}}\right)}{E_n\left(\mathbf{P_n}, \mathbf{X}^{\{l\}}, \mathbf{Y}^{\{l\}}\right)}$;
6: $n = n + 1$;
7: **until** $F(\chi(n)) < \epsilon_1$.
8: **Output:** $\mathbf{P}^{\{l+1\}} = \mathbf{P}(\mathbf{n})$.

B. UAV trajectory Optimization Design

The optimisation problem for the UAV trajectory can be solved as follows when the vehicle power allocation is obtained through the previous section. When the vehicle transmit power, denoted by $\left\{P_m^{\{l\}}\right\}$ and the time slot allocation for each iteration are given, the optimisation with respect to the UAV trajectory is described as follows:

$$\max_{\mathbf{Q}} = \frac{L_{m,R} + L_{m,U}(\mathbf{Q})}{E_m^{mec} + (1-\theta)E_{\mathrm{t}}^{R,\{l\}} + \theta E_{\mathrm{t}}^{U,\{l\}}} \tag{30}$$
$$\text{s.t. (14-2)} \tag{30-1}$$

the

$$L_{m,U}(\mathbf{Q}) = \log_2\left(1 + \frac{\varphi_{m,U}^{\{l\}}[t]}{\|q_M[t] - q_U[t]\| + H^2}\right) \tag{31}$$

Here, $\varphi_{m,U}^{\{l\}}[t] = \frac{p_m^{\{l\}}[t]\varsigma_0}{\sigma^2}$. The numerator part of the objective function of problem (30) is non-concave. We propose to approximate it by a continuous convex approximation method. In $q^{\{l\}}[t]$, the first-order Taylor expansion of the logarithmic form of the numerator part of Eq. (30) is performed as follows:

$$\log_2\left(1 + \frac{\varphi_{m,U}^{\{l\}}[t]}{\|q_M[t] - q_U[t]\| + H^2}\right) \tag{32}$$
$$\geq \left(\omega_m^{\{l\}}[t]\,\|q_M[t] - q_U[t]\|^2 - \left\|q_M[t] - q_U^{\{l\}}[t]\right\|^2 + \rho_m^{\{l\}}[t]\right)$$
$$\triangleq R_{m,U}^{\{l\}}(\mathbf{q}[t])$$

and,

$$\omega_m^{\{l\}}[t] = \frac{-\varphi_{m,U}^{\{l\}}[t]}{\ln 2\left(\left\|q_M[t] - q_U^{\{l\}}[t]\right\|^2 + H^2\right)} \cdot \frac{1}{\left\|q_M[t] - q_U^{\{l\}}[t]\right\|^2 + H^2 + \varphi_{m,U}^{\{l\}}[t]} \tag{33}$$

and,

$$\rho_m^{\{l\}}[t] = \log_2\left(1 + \frac{\varphi_{m,U}^{\{l\}}[t]}{\left\|q_M[t] - q_U^{\{l\}}[t]\right\| + H^2}\right) \tag{34}$$

The problem (30) is further transformed into:

$$\max_{\mathbf{Q}} = \frac{L_{m,R} + \sum_{t=1}^{T}\sum_{m=1}^{M} B_0 y_m^{\{l\}}[t]\,R_{m,U}^{\{l\}}(\mathbf{q}[t])}{E_m^{mec} + (1-\theta)E_{\mathrm{t}}^{R,\{l\}} + \theta E_{\mathrm{t}}^{U,\{l\}}} \tag{35}$$
$$\text{s.t. (14-2)} \tag{35-1}$$

At this point, the non-convex part of the problem (30) is transformed into a convex solvable form that can be solved using the convex optimisation toolbox CVX.

Algorithm 2 SCA-Based Algorithm for Trajectory Design

1: **Input:** Initialize variables $\mathbf{X}^{\{l\}}$, $\mathbf{Y}^{\{l\}}$and $\mathbf{P}^{\{l\}}$, set $n = 1$ as iteration index and $\epsilon_2 > 0$ as accuracy threshold.
2: **repeat**
3: Obtain $\mathbf{Q}_n = q_m[t]^*$ by solving (35) with $\mathbf{X}^{\{l\}}$, $\mathbf{X}^{\{l\}}$, $\mathbf{P}^{\{l\}}$ and ϵ_1.
4: Update the local points at the nth iteration as $R_{m,U}^{\{l\}}(\mathbf{q}[t]) = R_{m,U}^{\{l\}}(\mathbf{Q}[n])$;
5: $n = n + 1$;
6: **until** Converge to the prescribed accuracy ϵ_2.
7: **Output:** $\mathbf{Q}^{\{l+1\}} = \mathbf{Q}(\mathbf{n})$.

C. Subslot Resource Allocation Problems

From the inequality (14-4) with $A_{R,m} = z_m A_m$, we learn that the allocation of time slots is constrained by the server's computation time, and thus can be easily obtained:

$$z_m = \sum_{t=1}^{T} x_m[t], \qquad \forall m \in \mathcal{M} \tag{36}$$

This implies that the total duration of all time slots required for the vehicle to communicate with the terrestrial base station

is less than the vehicle's presence within the base station's coverage area. Once the power and trajectory parameters have been specified, the subproblem of time slot allocation can be formulated as follows:

$$\max_{\mathbf{X},\mathbf{Y}} = \frac{L_{m,R}(\mathbf{X}) + L_{m,U}(\mathbf{Y})}{E_m^{mec} + (1-\theta)E_{\mathrm{t}}^{R,\{l\}}(\mathbf{X}) + \theta E_{\mathrm{t}}^{U,\{l\}}(\mathbf{Y})} \quad (37)$$

$$\text{s.t. } (14\text{-}3), (14\text{-}4) \quad (37\text{-}1)$$

This is a fractional programming problem. We can use a Dinkelbach method to transform it into an easily solvable reduced-form programming problem. Equation (37) is equivalent to a linear programming problem that can be solved iteratively using the Convex Optimisation Toolbox (CVX).

D. Overall Algorithm Design

The original problem is divided into three subproblems, which are solved separately in the above subsections. They are then solved alternatively using an alternating iteration method, shown in Algorithm 3.

Algorithm 3 Power allocation and UAV trajectory optimization scheme based on Dinkelbach's method Algorithm

1: Initialize variables $\left\{\mathbf{P_m}^{\{l\}}\right\}$, $\left\{\mathbf{Q_m}^{\{l\}}\right\}$, $\left\{\mathbf{X_m}^{\{l\}}, \mathbf{Y_m}^{\{l\}}\right\}$, $\epsilon_3>0$ and let $l=1$.
2: **repeat**
3: Calculate the UAV's trajectory $\left\{\mathbf{Q_m}^{\{l+1\}}\right\}$ for given $\left\{\mathbf{P_m}^{\{l\}}\right\}$ and $\left\{\mathbf{X_m}^{\{l\}}, \mathbf{Y_m}^{\{l\}}\right\}$ by solving Algorithm 2;
4: Get the optimal power allocation $\left\{\mathbf{P_m}^{\{l\}}\right\}$ for given $\left\{\mathbf{Q_m}^{\{l\}}\right\}$ and $\left\{\mathbf{X_m}^{\{l\}}, \mathbf{Y_m}^{\{l\}}\right\}$ by solving Algorithm 1;
5: Solve the subslot scheduling $\left\{\mathbf{X_m}^{\{l\}}, \mathbf{Y_m}^{\{l\}}\right\}$ for given $\left\{\mathbf{P_m}^{\{l\}}\right\}$ and $\left\{\mathbf{Q_m}^{\{l\}}\right\}$ based on (37);
6: Update $l=l+1$.
7: **until** Converge to the prescribed accuracy ϵ_3.
8: **Output:** l,$p_m[t]^*$,$Q_m[t]^*$,$X_m[t]^*$.

Remark 1. *The computational complexity of algorithm 3 is analysed as follows. First, we focus on the inner loop. In step 3, the transformed UAV trajectory design problem is a linear program with T variables, so the complexity of step 3 is $\mathcal{O}\left(T^3 \log\left(1/\epsilon_2\right)\right)$. In step 4, the complexity of Dinkelbach's method is $\mathcal{O}\left(1/\epsilon_1^3 \log\left(MT\right)\right)$ [25], while each convex problem is solved by the Lagrange dual method with a complexity order of $\mathcal{O}\left(MT \log\left(1/\epsilon_3\right)\right)$. Similarly to step 4, Dinkelbach's method is used to solve the subslot scheduling problem in step 5, and the complexity to solve a linear problem at each iteration is $\mathcal{O}\left((MT)^3\right)$. We also assume that the BCD-based algorithm converges after L_c rounds in the outer loop. The total complexity of algorithm 3 is:*

$$\mathcal{O}\left(L_c\left(T^3 \log\left(\frac{1}{\epsilon_2}\right) + \frac{MT}{\epsilon_1^3}\log(MT)\log\left(\frac{1}{\epsilon_1}\right) + \frac{(MT)^3}{\epsilon_1^3}\log(MT)\right)\right)$$

IV. Simulation Results and Performance Analysis

In this section, we test the algorithms and evaluate their performance using numerical simulations. We mainly evaluate the performance of the joint optimisation of the UAV trajectory and the channel power allocation scheme. We present two schemes: the UAV hovering over a fixed position scheme and the way of fixing the UAV trajectory. We compare our scheme with them. In the hovering scheme, the UAV hovers above a fixed position to reduce the computational complexity. We simulate a two-way lane with a length of 3000 m and a width of 30 m. We select six vehicles for the simulation on the road, each travelling in a straight line at a constant speed with different speeds. The main parameters in the simulation are shown in Table II.

TABLE II: System parameters

Parameter	Value
Radio Range (R_a)	300 m
Carrier frequency (f_c)	5.9 GHz
CSI feedback period of vehicle (T)	1 ms
Average speed of vehicle	30 m/s
Mean of background noise (σ^2)	-30 dBm
Maximum transmitter power ($p_{i,max}$)	0.05 W
threshold parameter	10^{-6}
UAV flying altitude (H)	100 m
Number of slots (T)	80
RSU altitude (h_0)	5 m
Bandwidth of VUE channel (W)	10 MHz
UAV Maximum Flight Distance (V_{max})	2.5m
Pathloss exponent (θ)	4
Log-normal shadowing standard deviation	10 dB

Firstly, we show how to optimise the UAV trajectory to maximise the system's energy efficiency for different time slots. The black arrow represents the vehicle travelling to the right. We stipulate that the UAV flies from a fixed starting point to a fixed end point. When there's enough time, the UAV will stay close to the far vehicle to help it. Figure 3 shows the drone's speed at each time slot. When the vehicle needs help, the drone slows down or hovers to match the vehicle's speed.

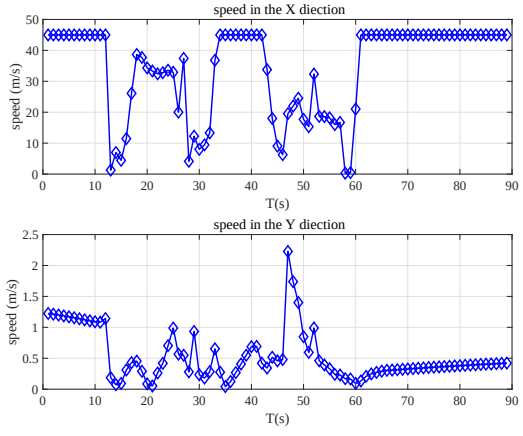

Fig. 3: UAV speed with different T

After testing the optimised algorithm, we tested the scheme with different parameters. Fig. 2 shows that different θ affect energy efficiency at different times. θ is a coefficient that compares energy costs at the drone and roadside units. When

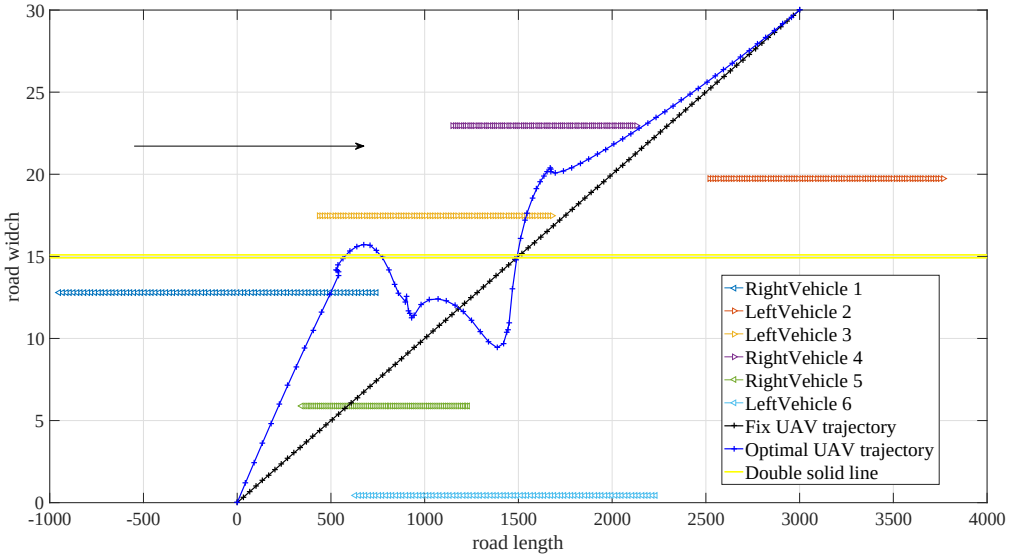

Fig. 2: UAVs trajectory for different T.

θ changes, the system utility also changes. Higher parameters mean more focus on the UAV's flight energy consumption. The overall system energy efficiency decreases as the UAV flight time T increases. Longer time allows the UAV to traverse more vehicles to obtain better channels and save energy. Lower θ leads to higher energy efficiency. This is because when we consider the UAV's energy consumption to be important, vehicles increase their power to transmit more data, thus increasing energy efficiency.

in environments with less time requirements, FPHS may be a more economical solution. However, FPHS is less energy efficient. The UAV hovers at a fixed position, which affects the efficiency of data transmission. As the flight cycle increases, the energy efficiency gap between OPTS and FPHS narrows. When the flight cycle is short, the OPTS has less time to send data to the UAV, so it uses less energy. As the flight cycle increases, the OPTS has more time to send data, so it uses more energy.

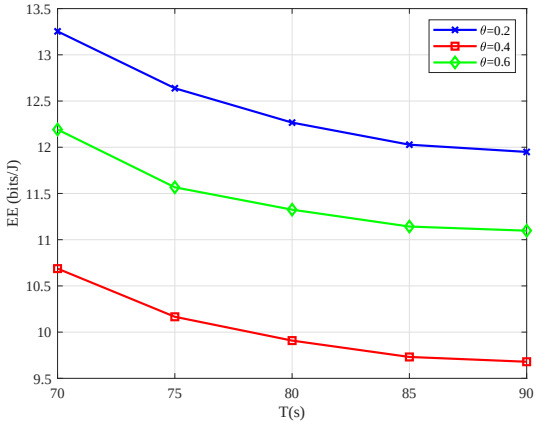

Fig. 4: EE versus collection time T with different θ

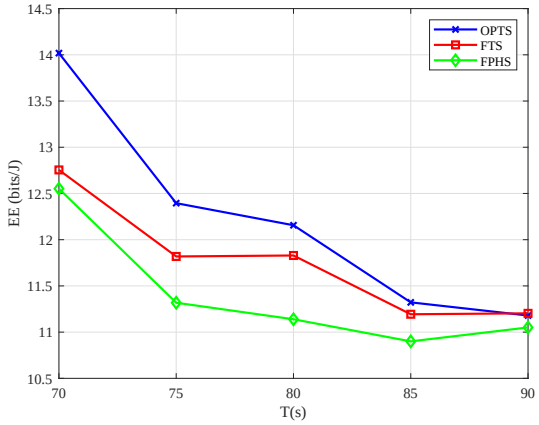

Fig. 5: EE of different schemes versus collection time T

Fig. 5 compares the energy efficiency of three UAV communication schemes, OPTS, FPHS and FTS, under different flight cycles T. As the UAV's flight time increases, each scheme's energy efficiency gradually stabilises. This is because the UAV has more time to transmit data at the right power. Further observation shows that the two schemes, OPTS and FPHS, are suitable for different scenarios. OPTS is better for situations where fast response is required. If the flight cycle is longer, FPHS is simpler to implement than OPTS. Therefore,

Fig. 6 shows how the energy efficiency of three UAV communication scenarios, OPTS, FHCS and FTS, varies with the parameter θ. The parameter θ reflects the weighting of the relative energy cost between the UAV's flight energy consumption and its communication energy consumption. When θ is large, the UAV's flight energy consumption is the main factor in overall energy consumption. The figure shows that as θ changes, the energy efficiency of all three scenarios decreases and reaches a low point at $\theta = 0.8$. It then increases slightly.

When θ is small, the UAV's flight energy consumption is low, so it can transmit data more. This improves energy efficiency. When θ is large, the UAV's flight energy consumption is high, so it can't transmit data, which affects energy efficiency. The parameter θ affects the energy efficiency of the three UAV communication schemes by influencing how much energy is used for flight and communication. In practice, we need to choose the right θ value for each situation to make UAV communication more efficient.

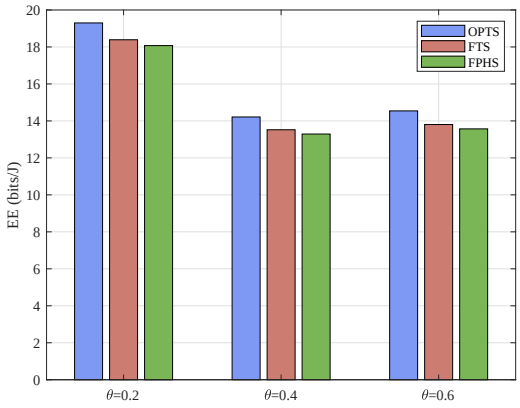

Fig. 6: EE of different schemes with different θ

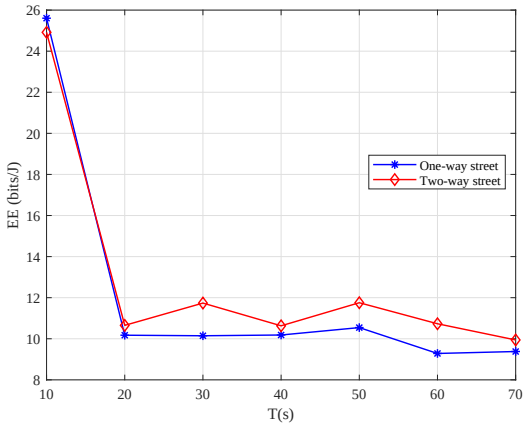

Fig. 7: twoway

Fig. 7 compares the two-way lane scenario with the one-way lane scenario. The two-way lane scenario is more energy efficient because it can use the roadside unit and airborne base station together more effectively.

V. Conclusions

In this paper, we propose an efficient air-ground integrated UAV-assisted vehicular communication scheme for two-way lanes. It also proposes a basic balancing scheme between throughput and energy consumption. By adjusting the vehicle's transmit power and the UAV's flight trajectory, as well as the allocation of time slots, the energy efficiency of the system can be maximised. This also ensures the quality of service of vehicular communication. Different parameters affect the energy efficiency of the system. By comparing different UAV flight scenarios, it can be seen that the UAV scenario with an optimised trajectory is the best. This chapter also looks at a more realistic scenario where roadside units and servers are often on one side of the road. In this case, vehicles driving away from the roadside unit cause communication difficulties. Using a drone to assist in communication could be a solution.

References

[1] W. Y. B. Lim, J. Huang, Z. Xiong, J. Kang, D. Niyato, X.-S. Hua, C. Leung, and C. Miao, "Towards Federated Learning in UAV-Enabled Internet of Vehicles: A Multi-Dimensional Contract-Matching Approach," *IEEE Transactions on Intelligent Transportation Systems*, vol. 22, no. 8, pp. 5140–5154, 2021.

[2] F. Liu, Z. Chen, and B. Xia, "Data dissemination with network coding in Two-Way Vehicle-to-Vehicle networks," *IEEE Transactions on Vehicular Technology*, vol. 65, no. 4, pp. 2445–2456, 2016.

[3] Z. Zhang, G. Mao, and B. D. O. Anderson, "On the information propagation process in mobile vehicular ad hoc networks," *IEEE Transactions on Vehicular Technology*, vol. 60, no. 5, pp. 2314–2325, 2011.

[4] E. Baccelli, P. Jacquet, B. Mans, and G. Rodolakis, "Highway vehicular delay tolerant networks: Information propagation speed properties," *IEEE Transactions on Information Theory*, vol. 58, no. 3, pp. 1743–1756, 2012.

[5] Z. Zhang, G. Mao, and B. D. O. Anderson, "Stochastic characterization of information propagation process in vehicular ad hoc networks," *IEEE Transactions on Intelligent Transportation Systems*, vol. 15, no. 1, pp. 122–135, 2014.

[6] H. Wu, R. M. Fujimoto, G. F. Riley, and M. Hunter, "Spatial propagation of information in vehicular networks," *IEEE Transactions on Vehicular Technology*, vol. 58, no. 1, pp. 420–431, 2009.

[7] H. Wu, F. Lyu, C. Zhou, J. Chen, L. Wang, and X. Shen, "Optimal UAV Caching and Trajectory in Aerial-Assisted Vehicular Networks: A Learning-Based Approach," *IEEE Journal on Selected Areas in Communications*, vol. 38, no. 12, pp. 2783–2797, 2020.

[8] F. Lyu, P. Yang, H. Wu, C. Zhou, J. Ren, Y. Zhang, and X. Shen, "Service-Oriented Dynamic Resource Slicing and Optimization for Space-Air-Ground Integrated Vehicular Networks," *IEEE Transactions on Intelligent Transportation Systems*, vol. 23, no. 7, pp. 7469–7483, 2022.

[9] J. Zhang, K. Han, P. Zhang, Z. Hou, and L. Ye, "A survey on joint-operation application for unmanned swarm formations under a complex confrontation environment," *Journal of Systems Engineering and Electronics*, vol. 34, no. 6, pp. 1432–1446, 2023.

[10] Z. Niu, X. S. Shen, Q. Zhang, and Y. Tang, "Space-Air-Ground integrated vehicular network for connected and automated vehicles: Challenges and solutions," *Intelligent and Converged Networks*, vol. 1, no. 2, pp. 142–169, 2020.

[11] W. Qi, Q. Song, L. Guo, and A. Jamalipour, "Energy-Efficient resource allocation for UAV-Assisted vehicular networks with spectrum sharing," *IEEE Transactions on Vehicular Technology*, vol. 71, no. 7, pp. 7691–7702, 2022.

[12] J. Du, Z. Kong, A. Sun, J. Kang, D. Niyato, X. Chu, and F. R. Yu, "Maddpg-based joint service placement and task offloading in mec empowered airground integrated networks," *IEEE Internet of Things Journal*, vol. 11, no. 6, pp. 10 600–10 615, 2024.

[13] X. Li, X. Du, N. Zhao, and X. Wang, "Computing over the sky: Joint uav trajectory and task offloading scheme based on optimization-embedding multi-agent deep reinforcement learning," *IEEE Transactions on Communications*, vol. 72, no. 3, pp. 1355–1369, 2024.

[14] A. Bansal, N. Agrawal, and K. Singh, "Rate-splitting multiple access for uav-based ris-enabled interference-limited vehicular communication system," *IEEE Transactions on Intelligent Vehicles*, vol. 8, no. 1, pp. 936–948, 2023.

[15] G. Yang, R. Dai, and Y.-C. Liang, "Energy-efficient uav backscatter communication with joint trajectory design and resource optimization," *IEEE Transactions on Wireless Communications*, vol. 20, no. 2, pp. 926–941, 2021.

[16] Z. Liu, J. Qi, Y. Shen, K. Ma, and X. Guan, "Maximizing energy efficiency in uav-assisted nomamec networks," *IEEE Internet of Things Journal*, vol. 10, no. 24, pp. 22 208–22 222, 2023.

[17] R. Aslani and E. Saberinia, "Energy-efficient power control and altitude planning for uav-based vehicular communications in 5g nr-v2x networks," *Transactions on Emerging Telecommunications Technologies*, vol. 34, no. 12, p. e4854, 2023.
[18] J. Wang, X. Zhou, H. Zhang, and D. Yuan, "Joint trajectory design and power allocation for uav assisted network with user mobility," *IEEE Transactions on Vehicular Technology*, vol. 72, no. 10, pp. 13 173–13 189, 2023.
[19] N. Kato, Z. M. Fadlullah, F. Tang, B. Mao, S. Tani, A. Okamura, and J. Liu, "Optimizing Space-Air-Ground Integrated Networks by Artificial Intelligence," *IEEE Wireless Communications*, vol. 26, no. 4, pp. 140–147, 2019.
[20] "Joint computation offloading and resource allocation in vehicular edge computing networks," *Digital Communications and Networks*, vol. 9, no. 6, pp. 1399–1410, 2023.
[21] F. Liu, Z. Chen, and B. Xia, "Data dissemination with network coding in two-way vehicle-to-vehicle networks," *IEEE Transactions on Vehicular Technology*, vol. 65, no. 4, pp. 2445–2456, 2016.
[22] M. Fiore and J. Härri, "The networking shape of vehicular mobility." New York, NY, USA: Association for Computing Machinery, 2008.
[23] Y. Xie, Z. Liu, K. Y. Chan, and X. Guan, "Energy-spectral efficiency optimization in vehicular communications: Joint clustering and pricing-based robust power control approach," *IEEE Transactions on Vehicular Technology*, vol. 69, no. 11, pp. 13 673–13 685, 2020.
[24] Y. Liang, L. Xiao, D. Yang, Y. Liu, and T. Zhang, "Joint trajectory and resource optimization for UAV-Aided Two-Way relay networks," *IEEE Transactions on Vehicular Technology*, vol. 71, no. 1, pp. 639–652, 2022.
[25] J.-P. Crouzeix and J. A. Ferland, "Algorithms for generalized fractional programming," *Mathematical Programming*, vol. 52, no. 1, pp. 191–207, 1991.